Received: 16 May 2024 | Revised: 9 July 2024 | Accepted: 29 July 2024

DOI: 10.1111/php.14019

RESEARCH ARTICLE

Spectroscopic analysis of bacterial photoreactivation

Keyvan Khosh Abady[1] | **Negar Karpourazar**[1] | **Arjun Krishnamoorthi**[1] | **Runze Li**[2] | **Peter M. Rentzepis**[1]

[1]Department of Electrical and Computer Engineering, Texas A&M University, College Station, Texas, USA

[2]School of Physical Science and Technology, Shanghai Tech University, Shanghai, China

Correspondence
Peter M. Rentzepis, Department of Electrical and Computer Engineering, Texas A&M University, College Station, TX, USA.
Email: prentzepis@tamu.edu

Funding information
Air Force Office of Scientific Research, Grant/Award Number: FA9550-20-1-0139

Abstract

With the rise of bacterial infections and antibiotic resistance, spectroscopic devices originally developed for bacterial detection have shown promise to rapidly identify bacterial strains and determine the ratio of live to dead bacteria. However, the detection of the photoreactivated pathogens remains a critical concern. This study utilizes fluorescence and Raman spectroscopy to analyze bacterial responses to UV irradiation and subsequent photoreactivation. Our experimental results reveal limitations in fluorescence spectroscopy for detecting photoreactivated bacteria, as the intense fluorescence of tryptophan and tyrosine amino acids masks the fluorescence emitted by thymine molecules. Conversely, Raman spectroscopy proves more effective, showing a detectable decrease in band intensities of *E. coli* bacteria at 1248 and 1665 cm^{-1} after exposure to UVC radiation. Subsequent UVA irradiation results in the partial restoration of these band intensities, indicating DNA repair and bacterial photoreactivation. This enhanced understanding aims to improve the accuracy and effectiveness of these spectroscopic tools in clinical and environmental settings.

KEYWORDS

DNA repair, fluorescence, photoreactivation, Raman, spectroscopy, UV inactivation

INTRODUCTION

The resurgence of bacterial infections has become one of the most significant health concerns around the world.[1] In 2019, nearly 13 million people died due to infections worldwide, and 7 million of those deaths were caused by bacterial infections.[2] The majority of this mortality is attributed to bacterial resistance to antibiotics.[3] The lack of rapid methods for the early detection of bacterial infections is one of the primary reasons for the overuse of antibiotics, which may lead to further bacterial resistance.[4–6] Therefore, there is an urgent need for the development of advanced diagnostic tools that can quickly and reliably identify bacterial infections.

The current traditional diagnostic methods for infectious bacteria include culturing the specimens on agar plates and counting the number of bacterial colonies formed.[7] This process usually takes several days due to the fact that many bacterial species have relatively slow growth rates, thus require a quite long time to form detectable colonies.[8] In addition, interpreting the results of these tests is usually difficult and requires expert laboratory

Abbreviations: DNA, Deoxyribonucleic acid; UV, ultraviolet.

personnel. Furthermore, a complicated sequence of tests is needed before confirmation of any diagnosis.[9] As a result, the time-consuming nature of these procedures can elevate the risk of more severe infections, which may lead to higher rates of mortality.[10]

To overcome this problem, extensive research has been carried out over the past few decades towards the development of novel devices that are capable of rapidly detecting bacterial infections, even at low concentrations.[11–13] Recently, spectroscopic techniques have been widely used as an alternative to traditional methods for bacterial detection owing to the fact that they are significantly faster, more sensitive, non-destructive, and relatively low-cost compared to the traditional methods.[14–18] In addition, these spectroscopic instruments are designed to work with various samples, including clinical specimens, and are used to detect bacterial contamination in food and water.[19–23]

In our earlier studies,[24,25] we have shown that the fluorescence spectra of bacterial samples or any other species can be recorded in situ within minutes by using our novel handheld fluorescence spectrometer. In addition, we have demonstrated that it is possible to determine the fraction of live to dead bacteria by inactivating these bacteria using UV irradiation or antibiotic treatment.[26] Furthermore, these tests can be performed on body fluids, including urine, saliva, or cerebrospinal fluid, to detect the presence of bacteria and enumerate them either by subjecting these fluids to UV radiation and determining the shift in the proportion of live to dead bacteria, or by monitoring the increasing number of inactivated bacteria following antibiotic treatment. In a separate study, we have also designed, constructed, and utilized a novel handheld Raman spectrometer,[27,28] which provides means for the rapid identification of bacterial strains, and determines the ratio of live to dead bacteria before and after UV irradiation. This is achieved by relying on the fact that the intensity of various vibrational bands in the Raman spectra of *E. coli* bacteria changes as a function of UV irradiation. For instance, a new Raman band is expected to be formed in the 1415 cm^{-1} region, which is linearly intensified as the duration of UV irradiation increases. We have demonstrated that the increase in the intensity of this band corresponds to the number of bacterial cells that have been inactivated by UV irradiation.

These spectroscopic devices find several applications, including the detection of bacterial pathogens that may present in different environments, such as drinking water,[29,30] wound effluents[31,32] and blood and urine samples from patients.[33–36] In addition, they are used to identify bacteria present in food, which can cause foodborne illnesses, in order to ensure that the food is safe to consume.[14,37–39] Furthermore, they can also be used as a tool for determining the effectiveness of various antibiotics in treating specific types of bacteria.[40–42]

However, the operational characteristics of such devices remain largely unknown under a range of conditions. Understanding how these devices function under such conditions is critical in order to ensure their reliability and effectiveness in clinical and environmental settings. One such condition is the photoreactivation of these bacteria after they have been inactivated by UV irradiation. This is due to the fact that photoreactivation can ultimately lead to an overestimation of the amount of pathogen removal.[43] For example, after UV irradiation for wound disinfection, the reactivation of pathogens can pose a significant risk, particularly if they remain undetected by spectroscopic or other means of bacterial detection. Similarly, the photoreactivation of these pathogens after water disinfection by UV irradiation is also a critical concern, especially if these photoreactivated bacteria remain undetected by the in-situ spectrometric devices used at various stages of the water testing process.[44–47] Therefore, the reliability and accuracy of these spectroscopic devices, used to detect pathogen reactivation, are crucial factors for assessing their overall utility and effectiveness.

In this article, we conducted a detailed study for a better understanding of the operational behavior and functionality of our previously developed handheld spectroscopic devices in the context of photoreactivation. These devices, originally designed for bacterial detection, are now being examined in order to determine whether they are capable of detecting the photoreactivated bacteria after inactivation by UVC irradiation. Using fluorescence and Raman spectroscopy, we expect to have a deeper insight into the mechanisms that govern the bacterial response to UV irradiation and the subsequent photoreactivation process. This is achieved through a comprehensive analysis of the recorded changes in the fluorescence spectra and Raman patterns of bacterial constituents.

Photoreactivation

The ultraviolet (UV) spectrum is divided into three main segments according to its distinct effects on biological samples[48–50]: UVA (320–400 nm), UVB (290–320 nm) and UVC (200–290 nm). Each of these irradiation energies induces different bacterial inactivation effects. For example, UVC and UVB radiation are known to cause damage to the genetic constituents (DNA and RNA) in the nucleus of microorganisms, including bacteria cells, thus preventing them from reproduction and growth.[27,51] This is affected by the absorption spectrum of the DNA molecules, which display two bands, one with a maximum around 200 nm and the other at 265 nm.[52] The

absorption of UVC photons by the thymine molecules inside the DNA results in the dimerization of the thymine molecules by producing cyclobutane dimers.[53] These dimers disrupt the base pairing process during DNA replication, preventing the bacterial cells from replication and consequently induces the effective death of these cells.[54] UVA radiation, while less directly damaging to DNA, profoundly influences aromatic amino acids present in protein structures, such as tryptophan and tyrosine. As a result, these amino acids undergo photooxidation, leading to the formation of reactive oxygen species (ROS) that inflict indirect damage upon bacteria, causing inactivation of their vital functions.[25,55–57]

However, UVA radiation also exhibits a different biological effect on bacterial cells. It has been shown that exposing bacteria to UVA radiation either simultaneously with UVC or following UVC irradiation reduces bacterial inactivation.[58] This is owing to the fact that the photolyase enzyme absorbs the energy of UVA, and dissociates the covalent bond formed between two adjacent thymine bases, and thus repairs the damaged DNA. This process is known as DNA photoreactivation.[59–61]

MATERIALS AND METHODS

Bacteria preparation and enumeration

The bacterium that is used for this study, *E. coli* K-12 strain, was provided to us by the Bacteriological Epidemiology and Antimicrobial Resistance unit of the USDA-ARS. These bacteria were grown in 10 mL of Luria Bertani (LB) broth (ThermoFisher) and incubated for 24 h at 37°C in accordance with the supplier's product instructions. After incubation, the bacteria were harvested by centrifugation (Fisher Scientific Model 228) at 3300 rpm for 5 min and then washed twice with 0.9% w/v saline solution in order to remove the growth medium. This step is necessary due to the fact that LB broth generates a significant fluorescence background during the spectroscopic measurements. Ultimately, bacterial samples were diluted in saline solution to the desired concentration of ~10^8 cells/mL before their absorption, emission, and Raman spectra were recorded.

In order to count bacterial colony forming units (CFU), bacterial solutions were collected after each UV irradiation time step and then serially diluted in saline to 1/10 concentrations. Subsequently, a 100 µL portion of each diluted bacterial solution was spread on tryptone soya agar (TSA) plates for bacterial growth. These plates were then placed on an incubator for 24 h at 37°C to enhance bacterial growth and ultimately, the plates with 10–100 colonies were selected for counting.

UV irradiation

In this study, deep UV irradiation was performed using a Qniceuvc model excimer lamp (60 W, 222 nm). This lamp was selected specifically for its ability to emit radiation at 222 nm, which has been proven to kill bacteria effectively, while remaining harmless to human cells.[62,63] The lamp exhibited a peak wavelength emission at 221.8 nm with an FWHM bandwidth of 4 nm. The UVA photoreactivation experiments were conducted using an LED, with a maximum wavelength emission at 368.5 nm (referred to as 365 nm) with an FWHM bandwidth of 12 nm. Figure 1 shows the emission spectra of both the excimer lamp and the 365 nm LED, recorded using an Ocean Optics USB2000+ spectrometer.

In order to accurately measure the power of the 222 nm radiation directed onto the sample, we employed a Thorlabs DET10A2 Si photodetector. The combination of this photodetector with the excimer lamp allowed for continuous monitoring of the 222 nm UV irradiation power density during our experiments.

In this work, a quartz cuvette with a high UV transmission and 1 cm pathlength was utilized to irradiate the bacterial solution with UV radiation. To ensure uniform exposure, a magnetic stirrer was used to maintain continuous mixing of the bacterial solution during UV irradiation.

The impact of bacterial inactivation on their fluorescence and Raman spectra was studied by subjecting bacterial samples to 222 nm irradiation with a power density of 9 µW/cm^2 for varying durations ranging from 30 s to 60 min for recording fluorescence spectra and 10 to 60 min for Raman spectra. Similarly, to test the effect of photoreactivation on both fluorescence and Raman

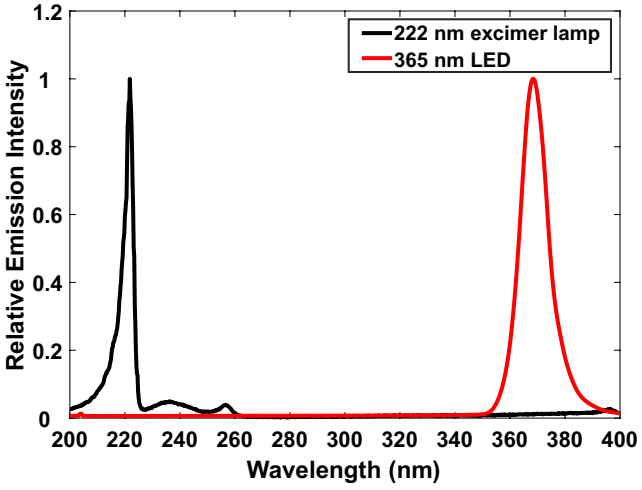

FIGURE 1 Emission spectra of the 222 nm excimer lamp and the 365 nm UV LED used in this study.

spectra, a 3 mL aliquot of the bacterial solution was initially inactivated by using 222 nm UV irradiation for 10 min to record the fluorescence spectra and 30 min for the Raman spectra. Subsequently, the samples were irradiated with a 365 nm LED radiation with a power density of 163 μW/cm^2 for different time durations, varying from 30 s to 1 h.

Spectroscopic measurements

The absorption, fluorescence, and Raman spectra were measured in a dark environment with dim red light at room temperature, before and after each UV irradiation time period. This precaution was taken due to the potential impact of ambient light on the inactivation and photoreactivation processes of bacteria.[64]

The absorption spectra were recorded by means of a Shimadzu 1201 UV–Vis spectrometer, while the emission spectra were recorded using a Shimadzu RF-5301 spectrofluorometer. In order to record fluorescence spectra, the excitation wavelength was set to 222 nm, which corresponds to nearly the maximum cross section of the absorption bands, unless otherwise stated.

Furthermore, a Horiba Xplora plus Raman spectrometer which is coupled to a microscope and a 25 mW, 638 nm laser were utilized to obtain the Raman spectra of the bacterial cells. The acquisition time was set to 100 s for each spectrum, and an average was taken from 10 spectra for every measurement. Initially, a 5 μL aliquot of the bacterial solution at a concentration of approximately 10^8 to 10^9 cells/mL, was placed on an aluminum mirror and immediately thereafter, the Raman spectra were recorded using a 10× objective lens of the microscope. As a result of recording spectra in wet condition, a prominent water band formed at 1650 cm^{-1}. This band, which corresponds to the vibrations of the OH bonding, was dominant, whereas the recorded Raman bands of bacterial cells were significantly weaker. To avoid this condition, the bacterial solution was centrifuged at 3300 rpm for 5 min to reach a concentration of approximately 10^{11} cells/mL. Subsequently, the supernatant was discarded, and a portion of 5 μL of the remaining bacterial pellets were dried on an aluminum mirror to record Raman spectra. To further enhance the intensity of the bacterial Raman spectra bands and improve the signal to noise ratio, a 100× microscope objective was used.

For each time period of UV irradiation, the absorption, fluorescence and Raman spectra were measured at least five times, and their averages were used for spectral interpretations.

RESULTS AND DISCUSSION

Effects of 222 and 365 nm irradiation on the inactivation and photoreactivation of the bacteria

Our study focused on the inactivation of bacteria using 222 nm irradiation and the subsequent photoreactivation of bacteria using 365 nm UV radiation. To that effect, the experimental data obtained from the inactivation experiments revealed a significant reduction in bacterial viability following exposure to 222 nm UV radiation, as shown in Figure 2A. Specifically, an irradiation dose of 16 mJ/cm^2 at 222 nm resulted in approximately a 4 log reduction in the *E. coli* bacterial population, which is consistent with the strong antimicrobial properties of 222 nm UVC radiation.[65]

Furthermore, our findings on the photoreactivation of bacteria using 365 nm UV irradiation after inactivation by 222 nm UV irradiation demonstrated a partial recovery of bacterial viability, as shown in Figure 2B. This observation is in agreement with prior studies on the photoreactivation of bacteria.[64]

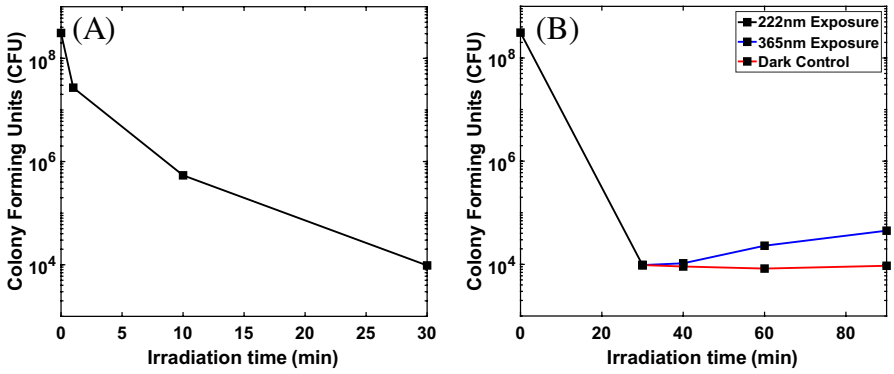

FIGURE 2 (A) Reduction in the *E. coli* bacterial population with respect to 222 nm UVC irradiation time. (B) Photoreactivation of *E. coli* bacteria using 365 nm UVA after initial inactivation with 222 nm irradiation.

Absorption, fluorescence and Raman spectra of *E. coli* bacteria

The absorption spectrum of the *E. coli* bacteria is shown in Figure 3. It has two prominent absorption bands with maximum intensities around 265 and 210 nm. These two bands, which mostly originated from the DNA component of the bacteria, specifically the thymine nucleotide base, have approximately the same absorption peaks.

Figure 4A shows the fluorescence spectrum of the *E. coli* bacteria, which is characterized by a broad band ranging from 280 to 500 nm and has a maximum intensity around 330 nm wavelength. This peak at 330 nm in the fluorescence spectra of *E. coli* bacteria mainly corresponds to the presence of tryptophan and tyrosine amino acids inside the bacteria. As a demonstration, Figure 4B,C show the synchronous fluorescence spectra of tyrosine and tryptophan in saline solution respectively, where the intensity maxima are observed at 310 nm for tyrosine and 350 nm for tryptophan. These spectra were recorded by utilizing the synchronous method, a technique that involves the simultaneous scanning of both the excitation and emission monochromators while a constant wavelength interval ($\Delta\lambda$) is maintained between the emission and excitation wavelengths throughout the scanning process. This approach enables us to selectively enhance a particular band of the fluorescence spectrum by choosing an appropriate $\Delta\lambda$ that corresponds to the difference in wavelength value of the intensity maxima between the absorption and fluorescence bands of the target fluorophore. Therefore, the fluorescence bands of tyrosine and tryptophan are distinctly separated and narrowed, as shown in Figure 4.

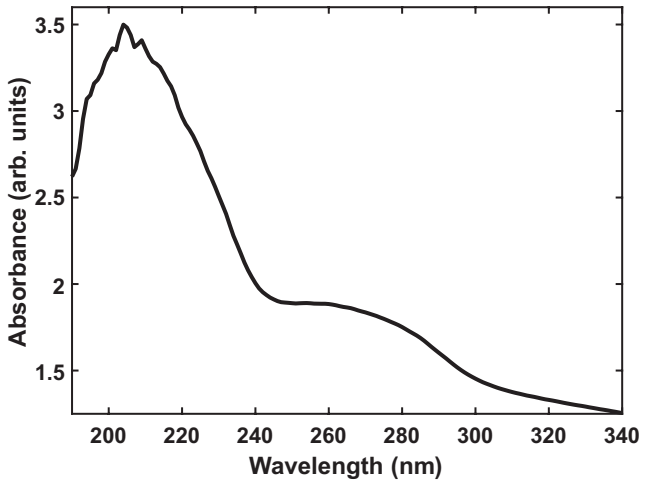

FIGURE 3 Absorption spectrum of *E. coli* bacteria measured at room temperature.

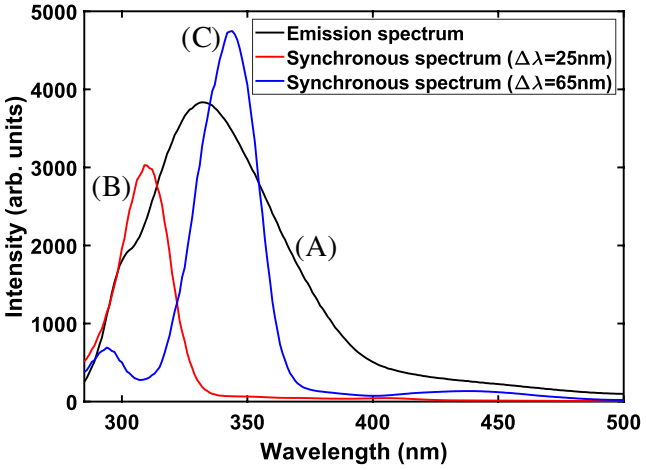

FIGURE 4 (A) Fluorescence spectrum of *E. coli* bacteria excited at 270 nm wavelength. (B) Synchronous spectrum of *E. coli* bacteria recorded with a $\Delta\lambda$ of 25 nm, depicts a distinct band at 310 nm that corresponds to tyrosine component. (C) Synchronous spectrum of *E. coli* bacteria recorded with a $\Delta\lambda$ of 65 nm, depicts a distinct band at 350 nm corresponds to tryptophan component.

Figure 4 further demonstrates that the bacterial fluorescence spectra are primarily composed of the spectra of the tryptophan and tyrosine components. Therefore, these two components in the fluorescence spectra of *E. coli* bacteria are more prominent than the spectra of other components, such as DNA.

Raman scattering offers a distinct spectroscopic signature of the chemical bonds present within a material. This is due to the fact that the vibrational modes of different chemical bonds result in an inelastic transition in the energy of the scattered photon. In the context of bacterial samples, Raman scattering can provide valuable information about different effects of UV exposure on various components inside bacteria. To that effect, Figure 5 shows the vibrational Raman spectra of the *E. coli* bacteria, with

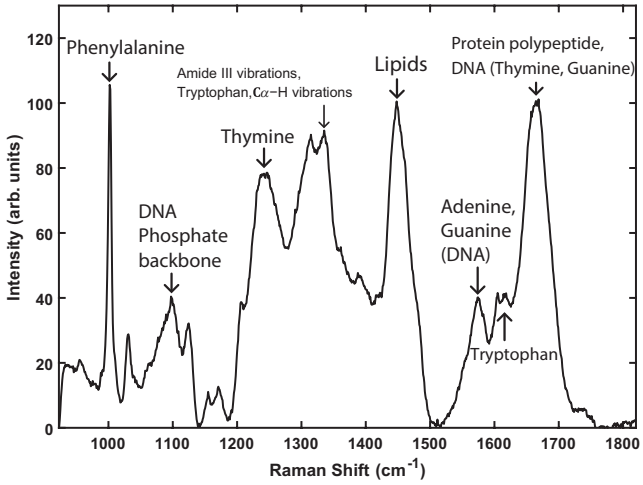

FIGURE 5 Vibrational Raman spectra of *E. coli* bacteria. Bands corresponding to different bacterial components are highlighted.

the bands corresponding to each bacterial component clearly indicated.

Effect of 222 nm excimer lamp irradiation on the fluorescence spectrum of *E. coli* bacteria

To determine the ratio of live to dead bacteria with respect to UV irradiation time using fluorescence spectroscopy technique, *E. coli* bacteria were exposed to $9\,\mu W/cm^2$, 222 nm UV irradiation for varying time durations, ranging from 0.5 to 60 min. The fluorescence spectra of the bacterial sample were obtained before and after each UV irradiation time step in order to determine the number of inactivated bacteria. To that effect, Figure 6A shows the variations in the fluorescence band intensity of *E. coli* bacterial cells versus UV exposure time. Furthermore, the change in the peak intensity at 330 nm with respect to 222 nm UV irradiation time is plotted in Figure 6B.

Figure 6 shows that as the *E. coli* bacteria is exposed to 222 nm UV radiation for a longer period of time, there is a continuous decrease in the intensity of the fluorescence band. This band is due to the tryptophan and tyrosine amino acids present in different protein structures inside the bacteria. As a result, Figure 6B shows the decay in the 330 nm maximum of the emission band of *E. coli* bacteria. This suggests that the decrease in this fluorescence band intensity corresponds to the decrease in tryptophan and tyrosine concentrations. The absorption of UV radiation by tryptophan and tyrosine amino acid components of the bacteria leads to their photodissociation, which in turn destroys the bacterial membrane. This can expose the intracellular components of the bacterial cell to UV radiation which results in the dimerization of DNA. This process disrupts the normal function of the cell and inhibits the replication of DNA, which ultimately results in bacterial inactivation. This phenomenon is shown in Figure 6, where a consistent decay in the maximum intensity of the fluorescence spectra from *E. coli* bacteria is clearly visible.

Effect of 222 nm excimer lamp irradiation on the Raman spectrum of *E. coli* bacteria

The vibrational Raman spectra of *E. coli* bacteria, recorded before and after each 222 nm UV exposure time period ranging from 0 to 60 min, are plotted in Figure 7. These spectra were recorded under dry condition, using the 100× Raman microscope objective lens, at a concentration of approximately 10^{11} cells/mL. Subsequently, the recorded spectra were normalized with respect to the band at $1450\,cm^{-1}$, which corresponds to the lipid components, for comparison.

After UV irradiation, a distinct band emerged at $1415\,cm^{-1}$, as shown in Figure 7. The peak intensity of this band at $1415\,cm^{-1}$ versus UV exposure time is illustrated in Figure 8A. This figure demonstrates that the band intensity exhibits a linear increase proportional to the dose of UV radiation. This band corresponds to protein photoproducts, and the intensity increase in this band correlates with the number of bacteria that have been inactivated by UV irradiation.

Figure 7 also provides further information regarding the effect of 222 nm UV irradiation on the other bacterial components. For example, Figures 7 and 8B reveal a detectable decrease in the Raman band intensity at $1248\,cm^{-1}$, which is indicative of degradation of thymine molecules due to UVC irradiation. Similarly, a decrease in the intensity of the $1665\,cm^{-1}$ band, as shown in Figures 7 and 8C, is found to be proportional to the formation of thymine dimers in the bacterial DNA.

In our earlier study,[61] the Raman spectra of thymine solutions before and after UV irradiation were recorded in order to detect the formation of thymine dimers. The current experimental results are in agreement with our previous findings.

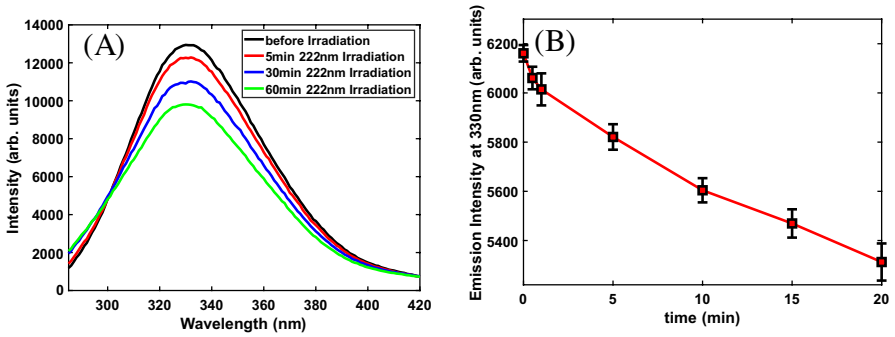

FIGURE 6 (A) Fluorescence spectra of *E. coli* bacteria before and after exposure to 222 nm UV radiation. (B) Fluorescence peak intensity variation at 330 nm as a function of 222 nm UV irradiation time.

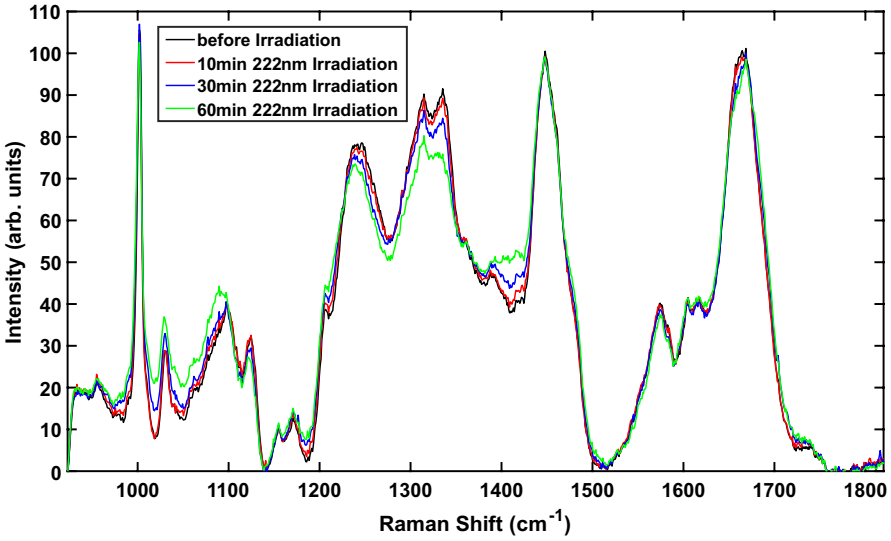

FIGURE 7 Normalized Raman spectra of *E. coli* bacteria before and after exposure to 222 nm UV radiation. The 1415 cm^{-1} band was formed as a result of UV irradiation.

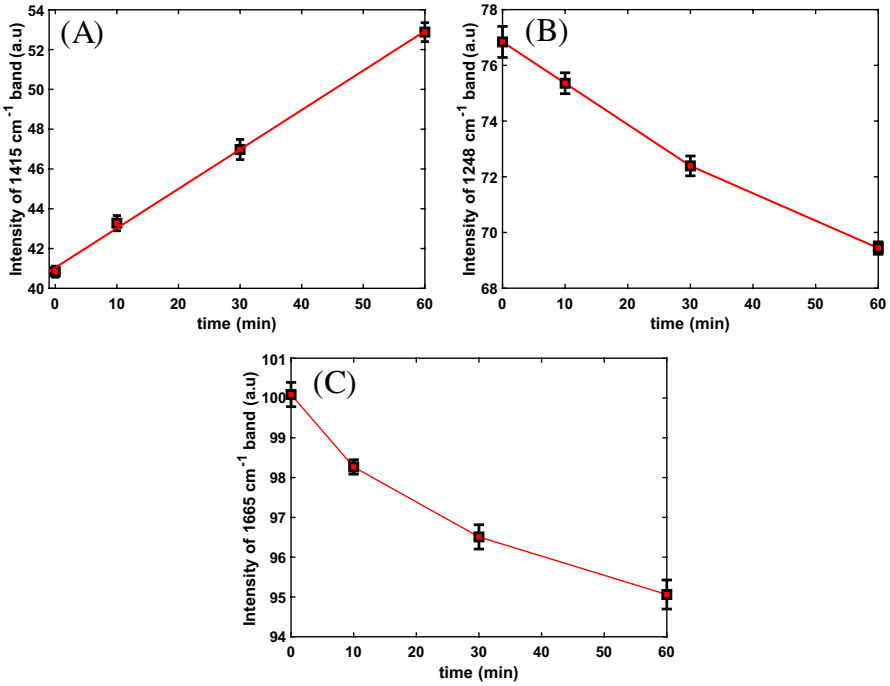

FIGURE 8 (A) Linear increase in the Raman intensity of *E. coli* bacteria at 1415 cm^{-1} and continuous decrease at (B) 1248 cm^{-1} and (C) 1665 cm^{-1} versus 222 nm UV irradiation time. The two bands at 1248 and 1665 cm^{-1} correspond to the vibrational bands of thymine molecules inside bacterial DNA.

Effect of photoreactivation on the fluorescence spectrum of *E. coli* bacteria

The fluorescence spectra of *E. coli* bacteria before and after 10 min of 222 nm UVC irradiation, followed by 365 nm UVA exposure, at various time intervals are plotted in Figure 9A. In addition, Figure 9B shows the variations in the fluorescence intensity maximum at 330 nm as a function of UV irradiation time.

The fluorescence intensity peak serves as an indicator of the bacteria concentration in the sample. Therefore, a decrease in intensity suggests a reduction in the number of viable bacteria per milliliter of saline solution, while an increase in the fluorescence peak intensity indicates an

increase in the number of viable bacteria.[24] Consequently, we expected a decrease in the fluorescence intensity peak after 222 nm irradiation due to the dimerization of thymine molecules inside DNA and inactivation of the bacteria. After 365 nm irradiation, followed by 222 nm exposure, we also expected to observe an increase in the fluorescence intensity maximum due to photoreactivation. However, it is evident from Figure 9A,B, that applying 365 nm irradiation followed by 222 nm irradiation, the fluorescence intensity peak decreases continuously. This is due to the fact that the changes in the intensity of this fluorescence band mostly correlate with the changes in tryptophan and tyrosine concentration rather than changes in DNA, because the fluorescing DNA component in the fluorescence spectrum is significantly weaker than tryptophan and tyrosine.

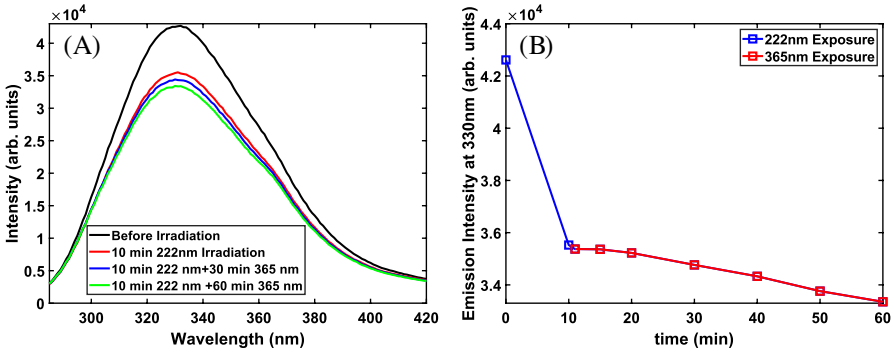

FIGURE 9 (A) Fluorescence spectra of *E. coli* bacteria in saline solution irradiated with 222 and 365 nm UV radiation. (B) Fluorescence peak intensity changes at 330 nm as a function of 222 and 365 nm irradiation time.

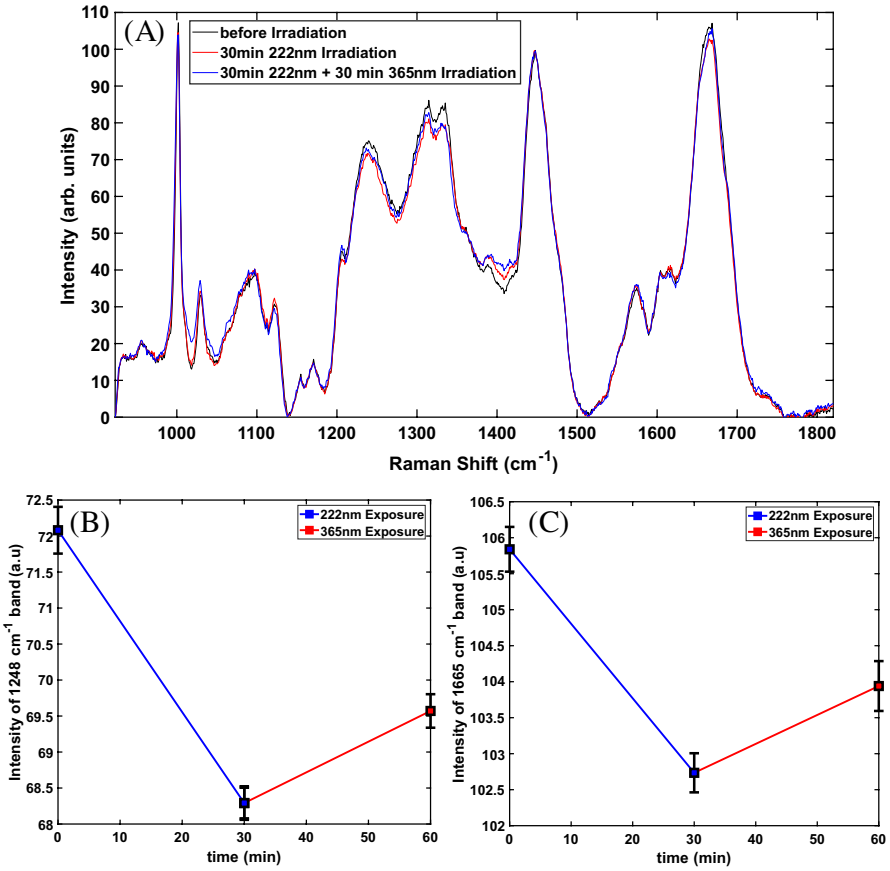

FIGURE 10 (A) Raman spectra of *E. coli* bacteria before and after exposure to 222 and 365 nm. Raman intensity variations at (B) 1248 cm^{-1} and (C) 1665 cm^{-1} corresponding to the vibrational band of thymine molecule inside bacterial DNA, with respect to the 222 and 365 nm irradiation time.

This experiment was conducted five times, with a fixed initial dose of 222 nm UV radiation and varying doses of 365 nm radiation, ranging from 1.63 to 587 mJ/cm^2. In all of these experiments, the fluorescence bands were found to decay continuously after being subjected to 365 nm irradiation, followed by 222 nm UV exposure.

As a result, utilizing fluorescence spectroscopy for bacteria identification in various environments may pose a significant risk because the photoreactivated bacteria will remain undetected by these devices. This may ultimately result in an overestimation of pathogen removal and pose a potential threat to public health.

Effect of photoreactivation on the Raman spectrum of *E. coli* bacteria

The Raman spectra of *E. coli* bacteria after 30 min of 365 nm irradiation, followed by 222 nm UV irradiation, are plotted in Figure 10A. These spectra were recorded under dry condition, using the 100× objective lens of the Raman microscope and normalized to the lipid band at 1450 cm^{-1}.

Upon close examination of the results presented in Figure 10A, we identified various changes in the Raman vibrations of several bacterial components as a result of UV irradiation. For example, a small decrease in the 1665 and 1248 cm^{-1} band intensities after 30 min of 222 nm irradiation is observed, which is the result of the dimerization of thymine bases inside DNA molecules. By irradiating the sample with 365 nm after 222 nm irradiation, the covalent bond formed between two adjacent thymine bases dissociates and results in the repair of the damaged DNA. Consequently, the band maximum intensities at 1248 and 1665 cm^{-1} increase, as shown in Figure 10B,C, respectively.

From the experimental data presented in this section, we can conclude that the handheld Raman spectrometer used for monitoring the changes in band intensity at 1248 and 1665 cm^{-1}, enables us not only to identify the ratio of live to dead bacterial cells, but also to detect the bacteria that have undergone photoreactivation as a consequence of UVA exposure.

CONCLUSION

In this study, we have made significant progress in understanding bacterial responses to UV irradiation and subsequent photoreactivation. This research provided insights on the spectral changes and vibrational patterns in bacterial constituents due to the irradiation of UVC and UVA, using fluorescence and Raman spectroscopy. We have identified the limitations of fluorescence spectroscopy in detecting photoreactivated bacteria, which could potentially lead to an overestimation of pathogen removal and pose a threat to public health. However, we show that Raman spectroscopy has proven to be more effective, enabling us to identify not only the ratio of live to dead bacterial cells but also detect bacteria that have undergone photoreactivation as a consequence of UVA exposure. These findings are crucial for improving the reliability and effectiveness of spectroscopic devices in clinical and environmental settings, particularly in cases that involve UV irradiation for disinfection purposes. Our future research will focus on further improving these spectroscopic tools to enhance their accuracy in detecting photoreactivated pathogens, contributing to broader efforts in combating bacterial infections and antibiotic resistance.

AUTHOR CONTRIBUTIONS

K.K. and P.M.R. designed research; P.M.R. supervised project and K.K. performed research; K.K. and P.M.R. and N.K. analyzed data; K.K. wrote initial draft of manuscript; K.K. and P.M.R. and R.L. and N.K. and A.K. revised the initial draft of manuscript; funding acquisition by P.M.R. All authors have read and agreed to the final version of the manuscript.

ACKNOWLEDGMENTS

This study was supported by Air Force Office of Scientific Research (AFOSR) Grant number FA9550-20-1-0139 and Texas A&M Engineering Experiment Station (TEES) funds.

CONFLICT OF INTEREST STATEMENT

The authors declare no competing interests.

ORCID

Keyvan Khosh Abady https://orcid.org/0000-0002-8558-824X
Negar Karpourazar https://orcid.org/0000-0001-9320-9716
Arjun Krishnamoorthi https://orcid.org/0000-0002-9764-4990

REFERENCES

1. Wu ZL, Zhao J, Xu R. Recent advances in oral nano-antibiotics for bacterial infection therapy. *Int J Nanomedicine*. 2020;15:9587-9610.
2. Ikuta KS, Swetschinski LR, Aguilar GR, et al. Global mortality associated with 33 bacterial pathogens in 2019: a systematic analysis for the Global Burden of Disease Study 2019. *Lancet*. 2022;400:2221-2248.
3. Murray CJ, Ikuta KS, Sharara F, et al. Global burden of bacterial antimicrobial resistance in 2019: a systematic analysis. *Lancet*. 2022;399:629-655.

4. Yee E, Cheng S, Knappe G, Moomau C. Antibiotic resistance: how to prevent the next public health emergency. *MIT Sci Policy Rev*. 2020;1:10-17.
5. Vasala A, Hytonen VP, Laitinen OH. Modern tools for rapid diagnostics of antimicrobial resistance. *Front Cell Infect Microbiol*. 2020;10:308.
6. O'Neill J. Tackling drug-resistant infections globally: final report and recommendations. 2016. Published by Government of the United Kingdom. https://apo.org.au/node/63983 Accessed June 24, 2024.
7. Rajapaksha P, Elbourne A, Gangadoo S, Brown R, Cozzolino D, Chapman J. A review of methods for the detection of pathogenic microorganisms. *Analyst*. 2019;144:396-411.
8. King MD, Lacey RE, Pak H, et al. Assays and enumeration of bioaerosols-traditional approaches to modern practices. *Aerosol Sci Tech*. 2020;54:611-633.
9. Ivnitski D, Abdel-Hamid I, Atanasov P, Wilkins E. Biosensors for detection of pathogenic bacteria. *Biosens Bioelectron*. 1999;14:599-624.
10. Şen Karaman D, Ercan UK, Bakay E, Topaloğlu N, Rosenholm JM. Evolving technologies and strategies for combating antibacterial resistance in the advent of the postantibiotic era. *Adv Funct Mater*. 2020;30:1908783.
11. Ezenarro JJ, Mas J, Munoz-Berbel X, Uria N. Advances in bacterial concentration methods and their integration in portable detection platforms: a review. *Anal Chim Acta*. 2022;1209:339079.
12. Reali S, Najib EY, Treuerne Balazs KE, et al. Novel diagnostics for point-of-care bacterial detection and identification. *RSC Adv*. 2019;9:21486-21497.
13. Gao D, Ma Z, Jiang Y. Recent advances in microfluidic devices for foodborne pathogens detection. *TrAC Trends Anal Chem*. 2022;157:116788.
14. Petersen M, Yu Z, Lu X. Application of Raman spectroscopic methods in food safety: a review. *Biosensors*. 2021;11:187.
15. Ferone M, Gowen A, Fanning S, Scannell AGM. Microbial detection and identification methods: bench top assays to omics approaches. *Compr Rev Food Sci Food Saf*. 2020;19:3106-3129.
16. McGoverin C, Steed C, Esan A, Robertson J, Swift S, Vanholsbeeck F. Optical methods for bacterial detection and characterization. *APL Photon*. 2021;6(8).
17. Pandian S, Lakshmi SA, Priya A, et al. Spectroscopic methods for the detection of microbial pathogens and diagnostics of infectious diseases—an updated overview. *Processes*. 2023;11:1191.
18. Liu L, Ma W, Wang X, Li S. Recent progress of surface-enhanced Raman spectroscopy for bacteria detection. *Biosensors*. 2023;13:350.
19. Nnachi RC, Sui N, Ke B, et al. Biosensors for rapid detection of bacterial pathogens in water, food and environment. *Environ Int*. 2022;166:107357.
20. Sohrabi H, Majidi MR, Khaki P, Jahanban-Esfahlan A, de la Guardia M, Mokhtarzadeh A. State of the Art: Lateral flow assays toward the point-of-care foodborne pathogenic bacteria detection in food samples. *Compr Rev Food Sci Food Saf*. 2022;21:1868-1912.
21. Ho CS, Jean N, Hogan CA, et al. Rapid identification of pathogenic bacteria using Raman spectroscopy and deep learning. *Nat Commun*. 2019;10:4927.
22. Chen W, Yao Y, Chen T, Shen W, Tang S, Lee HK. Application of smartphone-based spectroscopy to biosample analysis: a review. *Biosens Bioelectron*. 2021;172:112788.
23. Neugebauer U, Rosch P, Popp J. Raman spectroscopy towards clinical application: drug monitoring and pathogen identification. *Int J Antimicrob Agents*. 2015;46(Suppl 1):S35-S39.
24. Li R, Goswami U, King M, Chen J, Cesario TC, Rentzepis PM. In situ detection of live-to-dead bacteria ratio after inactivation by means of synchronous fluorescence and PCA. *Proc Natl Acad Sci USA*. 2018;115:668-673.
25. Li R, Dhankhar D, Chen J, Cesario TC, Rentzepis PM. A tryptophan synchronous and normal fluorescence study on bacteria inactivation mechanism. *Proc Natl Acad Sci USA*. 2019;116:18822-18826.
26. Li R, Dhankhar D, Chen J, Cesario TC, Rentzepis PM. Determination of live:dead bacteria as a function of antibiotic treatment. *J Microbiol Methods*. 2018;154:73-78.
27. Li R, Dhankhar D, Chen J, Krishnamoorthi A, Cesario TC, Rentzepis PM. Identification of live and dead bacteria: a Raman spectroscopic study. *IEEE Access*. 2019;7:23549-23559.
28. Dhankhar D, Nagpal A, Rentzepis PM. Cell-phone camera Raman spectrometer. *Rev Sci Instrum*. 2021;92:054101.
29. Kusic D, Kampe B, Rosch P, Popp J. Identification of water pathogens by Raman microspectroscopy. *Water Res*. 2014;48:179-189.
30. van de Vossenberg J, Tervahauta H, Maquelin K, et al. Identification of bacteria in drinking water with Raman spectroscopy. *Anal Methods*. 2013;5:2679-2687.
31. Ghebremedhin M, Yesupriya S, Crane NJ. Surface enhanced Raman spectroscopy as a point-of-care diagnostic for infection in wound effluent. Vol. 9715, pp. 43–50. SPIE, Proceedings of the Optical Diagnostics and Sensing XVI: Toward Point-of-Care Diagnostics. 2016.
32. Crane NJ, Elster EA. Profiling wound healing with wound effluent: Raman spectroscopic indicators of infection. Vol. 8220, pp. 96–103. SPIE, Proceedings of the Optical Biopsy X. 2012.
33. Wang L, Liu W, Tang JW, et al. Applications of Raman spectroscopy in bacterial infections: principles, advantages, and shortcomings. *Front Microbiol*. 2021;12:683580.
34. Pahlow S, Meisel S, Cialla-May D, Weber K, Rosch P, Popp J. Isolation and identification of bacteria by means of Raman spectroscopy. *Adv Drug Deliv Rev*. 2015;89:105-120.
35. Boardman AK, Wong WS, Premasiri WR, et al. Rapid detection of bacteria from blood with surface-enhanced Raman spectroscopy. *Anal Chem*. 2016;88:8026-8035.
36. Rusciano G, Capriglione P, Pesce G, Abete P, Carnovale V, Sasso A. Raman spectroscopy as a new tool for early detection of bacteria in patients with cystic fibrosis. *Laser Phys Lett*. 2013;10:075603.
37. Saravanan A, Kumar PS, Hemavathy RV, et al. Methods of detection of food-borne pathogens: a review. *Environ Chem Lett*. 2020;19:189-207.
38. Huayhongthong S, Khuntayaporn P, Thirapanmethee K, Wanapaisan P, Chomnawang MT. Raman spectroscopic analysis of food-borne microorganisms. *LWT*. 2019;114:108419.
39. Shen Y, Zhang Y, Gao ZF, et al. Recent advances in nanotechnology for simultaneous detection of multiple pathogenic bacteria. *Nano Today*. 2021;38:101121.
40. Munchberg U, Rosch P, Bauer M, Popp J. Raman spectroscopic identification of single bacterial cells under antibiotic influence. *Anal Bioanal Chem*. 2014;406:3041-3050.

41. Lu X, Al-Qadiri HM, Lin M, Rasco BA. Application of mid-infrared and Raman spectroscopy to the study of bacteria. *Food Bioproc Tech*. 2011;4:919-935.
42. Han YY, Lin YC, Cheng WC, et al. Rapid antibiotic susceptibility testing of bacteria from patients' blood via assaying bacterial metabolic response with surface-enhanced Raman spectroscopy. *Sci Rep*. 2020;10:12538.
43. Maghsoodi M, Lowry GL, Smith IM, Snow SD. Evaluation of parameters governing dark and photo-repair in UVC-irradiated *Escherichia coli*. *Environ Sci Water Res Technol*. 2022;8:407-418.
44. Wang M, Ateia M, Awfa D, Yoshimura C. Regrowth of bacteria after light-based disinfection – what we know and where we go from here. *Chemosphere*. 2021;268:128850.
45. Zimmer JL, Slawson RM. Potential repair of *Escherichia coli* DNA following exposure to UV radiation from both medium- and low-pressure UV sources used in drinking water treatment. *Appl Environ Microbiol*. 2002;68:3293-3299.
46. Henderson RK, Baker A, Murphy KR, Hambly A, Stuetz RM, Khan SJ. Fluorescence as a potential monitoring tool for recycled water systems: a review. *Water Res*. 2009;43:863-881.
47. Zulkifli SN, Rahim HA, Lau WJ. Detection of contaminants in water supply: a review on state-of-the-art monitoring technologies and their applications. *Sens Actuat B Chem*. 2018;255:2657-2689.
48. Matts PJ. Solar ultraviolet radiation: definitions and terminology. *Dermatol Clin*. 2006;24:1-8.
49. Romanhole RC, Ataide JA, Moriel P, Mazzola PG. Update on ultraviolet A and B radiation generated by the sun and artificial lamps and their effects on skin. *Int J Cosmet Sci*. 2015;37:366-370.
50. Vázquez M, Hanslmeier A. *Ultraviolet Radiation in the Solar System*. Springer; 2005.
51. Rastogi RP, Richa A, Tyagi KMB, Sinha RP. Molecular mechanisms of ultraviolet radiation-induced DNA damage and repair. *J Nucleic Acids*. 2010;2010:592980.
52. Kalisvaart BF. Re-use of wastewater: preventing the recovery of pathogens by using medium-pressure UV lamp technology. *Water Sci Technol*. 2004;50:337-344.
53. Paul D, Mu H, Zhao H, et al. Structure and mechanism of pyrimidine-pyrimidone (6-4) photoproduct recognition by the Rad4/XPC nucleotide excision repair complex. *Nucleic Acids Res*. 2019;47:6015-6028.
54. Nelson DL, Cox MM. *Lehninger Principles of Biochemistry*. International edition. W.H. Freeman; 2017.
55. Williams PD, Eichstadt SL, Kokjohn TA, Martin EL. Effects of ultraviolet radiation on the gram-positive marine bacterium *Microbacterium maritypicum*. *Curr Microbiol*. 2007;55:1-7.
56. Bolton NF, Cromar NJ, Hallsworth P, Fallowfield HJ. A review of the factors affecting sunlight inactivation of microorganisms in waste stabilisation ponds: preliminary results for enterococci. *Water Sci Technol*. 2010;61:885-890.
57. Sun W, Jing Z, Zhao Z, et al. Dose-response behavior of pathogens and surrogate microorganisms across the ultraviolet-C spectrum: inactivation efficiencies, action spectra, and mechanisms. *Environ Sci Technol*. 2023;57:10891-10900.
58. Song K, Mohseni M, Taghipour F. Mechanisms investigation on bacterial inactivation through combinations of UV wavelengths. *Water Res*. 2019;163:114875.
59. Kao Y-T, Saxena C, Wang L, Sancar A, Zhong D. Direct observation of thymine dimer repair in DNA by photolyase. *Proc Natl Acad Sci USA*. 2005;102:16128-16132.
60. Heelis PF, Kim S-T, Okamura T, Sancar A. New trends in photobiology: the photo repair of pyrimidine dimers by DNA photolyase and model systems. *J Photochem Photobiol B Biol*. 1993;17:219-228.
61. Nagpal A, Dhankhar D, Cesario TC, Li R, Chen J, Rentzepis PM. Thymine dissociation and dimer formation: a Raman and synchronous fluorescence spectroscopic study. *Proc Natl Acad Sci USA*. 2021;118:e2025263118.
62. Buonanno M, Ponnaiya B, Welch D, et al. Germicidal efficacy and mammalian skin safety of 222-nm UV light. *Radiat Res*. 2017;187:483-491.
63. Narita K, Asano K, Naito K, et al. Ultraviolet C light with wavelength of 222 nm inactivates a wide spectrum of microbial pathogens. *J Hosp Infect*. 2020;105:459-467.
64. Song K, Taghipour F, Mohseni M. Microorganisms inactivation by wavelength combinations of ultraviolet light-emitting diodes (UV-LEDs). *Sci Total Environ*. 2019;665:1103-1110.
65. Kang JW, Lee JI, Jeong SY, Kim YM, Kang DH. Effect of 222-nm krypton-chloride excilamp treatment on inactivation of *Escherichia coli* O157:H7 and Salmonella Typhimurium on alfalfa seeds and seed germination. *Food Microbiol*. 2019;82:171-176.

How to cite this article: Abady KK, Karpourazar N, Krishnamoorthi A, Li R, Rentzepis PM. Spectroscopic analysis of bacterial photoreactivation. *Photochem Photobiol*. 2025;101:494-504. doi:10.1111/php.14019